Kinetic Study of the Recombination Reaction of Gas Phase Pd(a^1S_0) with O_2 from 294 to 523 K

Mark L. Campbell*

Chemistry Department, United States Naval Academy, Annapolis, Maryland 21402

John M. C. Plane

School of Environmental Sciences, University of East Anglia, Norwich, NR4 7TJ, United Kingdom

Received: September 20, 2002; In Final Form: February 26, 2003

The gas-phase removal rate constants for the reaction of ground-state palladium (a^1S_0) with oxygen in argon buffer are reported as a function of temperature and pressure. Palladium atoms were produced by the photodissociation of palladium(II) trifluoroacetate and detected by laser-induced fluorescence. The reaction is pressure dependent, indicating recombination to form PdO_2. Falloff behavior is observed at pressures above about 20 Torr. Quantum calculations indicate that the reaction proceeds on a triplet surface to form bent $PdO_2(^3A'')$, which has a low frequency bending mode of only 129 cm^{-1} and a bond energy $D_0 = 95$ kJ mol^{-1}. RRKM theory, fitted to the experimental data, shows that D_0 should lie below 155 kJ mol^{-1} and predicts the following expression for the rate coefficient from 200 to 600 K: $k_{rec,0} = 1.09 \times 10^{-30}$ $(T/300\ K)^{-2.76}$ cm^6 $molecule^{-2}$ s^{-1}, $k_{rec,\infty} = 2.52 \times 10^{-10}$ $\exp(-69.3/T)$ cm^3 $molecule^{-1}$ s^{-1}, and $F_c = 0.61$.

Introduction

Studies of temperature-dependent rate constants for the main group, lanthanide and transition metal reactions with O_2 in the gas phase have been extensive.[1−23] Atmospheric scientists are interested in these reactions due to the presence of metallic species in the atmosphere from meteor ablation[24,25] and pollution from industrial smokestacks.[26]

The mechanism for the reaction of a gas-phase metal atom with oxygen is dependent upon the thermodynamics of the process. About half of the naturally occurring metals are able to exothermically abstract an oxygen atom to form the metal monoxide. In the cases in which the abstraction process is exothermic, the abstraction channel is the observed mechanism while the reaction barriers are observed to be 15 kJ/mol or less.[1−10] For the abstraction reactions involving transition metal reactions, it has been observed that those metals with s^1d^{n-1} configurations exhibit lower barriers than those with s^2d^{n-2} configurations.[7] For the lanthanides, it was found that the energy barrier for the abstraction of an oxygen atom to produce the metal oxide was related to the s^2 to s^1 promotion energy of the lanthanide metal atom.[9] Thus, for the oxygen abstraction reactions the electronic structure of the reactant metal atom has a dramatic effect on the dynamics of these reactions.

For many gas-phase metal atoms, the abstraction reaction is endothermic. Thus, at moderate temperatures recombination with O_2 to produce the metal dioxide is the only feasible process. This is the case for the main group metals (with the exception of Ba, Al, Ge, and Sn), about half of the transition metals, and one of the lanthanides (Yb). The kinetics of the recombination reactions involving these atoms are quite diverse. Brown et al reported on the 3d transition metal series and found that atoms with a ground or low-lying electronic state with a single electron in the valence s subshell react faster than those metals atoms with ground states with a filled outer s subshell.[11] This behavior has also generally been observed for the 4d and 5d transition metal series,[14−17] although unpublished results from our laboratory indicate silver ($k_{rec,o} < 2 \times 10^{-34}$ cm^6 $molecule^{-2}$ s^{-1}) and gold ($k_{rec,o} < 4 \times 10^{-35}$ cm^6 $molecule^{-2}$ s^{-1}) are quite unreactive with O_2 despite their s^1 ground-state configurations. In the case of the alkaline earths, iron and ytterbium, the termolecular reaction rate coefficients exhibit an unusual positive temperature dependence which has been attributed to the repulsion associated with a filled s valence subshell.[9,18−23] Again, the electronic structure of the metal atoms plays an important role in the dynamics of these recombination reactions.

It is widely recognized that palladium is the most versatile metal in promoting or catalyzing reactions, particularly those involving carbon−carbon bond formation.[27] The interaction of small gas molecules with bulk palladium is currently an active area of research, such as the reduction of O_2 on palladium electrode surfaces in fuel cells.[28] Palladium with its $[Kr]4d^{10}$ ground-state configuration is unique among the transition metals due to its empty valence s subshell. The formation of η^2-complexes with hydrocarbons, unique among the transition metals, has been attributed to its empty s subshell ground-state configuration.[29,30] The unusually weak bond in the PdO molecule has also been attributed to palladium's unique electronic structure.[31] The abstraction channel to form PdO is endothermic by 220 kJ mol^{-1} so that the abstraction process is expected to be unimportant at ordinary temperatures.[32] Here we report an experimental study of the recombination reaction of ground-state palladium with O_2. Quantum calculations on PdO_2 are then described which provide the input for a RRKM fit to the experimental rate constants.

Experimental Section

Pseudo first-order kinetic experiments ($[Pd] \ll O_2]$) were performed in an apparatus with slowly flowing gas using a laser photolysis/laser-induced fluorescence (LIF) technique. The experimental apparatus and technique have been described in

10.1021/jp022116i CCC: $25.00
Published on Web 04/12/2003

detail elsewhere.[33] Briefly, the reaction chamber is a stainless steel reducing four-way cross with attached sidearms and a sapphire window for optical viewing. The reaction chamber is enclosed within a convection oven (Blue M, model 206F, T_{max} = 623 K) with holes drilled to allow for the exiting sidearms and the telescoping of the LIF signal to the PMT. Palladium atoms were produced via 248 nm photodissociation of palladium(II) trifluoroacetate [$Pd(CF_3CO_2)_2$] using the output of an excimer laser (Lambda Physics Lextra 200). The palladium atoms were detected via LIF using an excimer-pumped dye laser (Lambda Physics Lextra 50/ScanMate 2E). Detection of palladium atoms was accomplished by exciting the 5p $^3D_1^\circ - a^1S_0$ transition at 247.642 nm and detecting the 5p $^3D_1^\circ - 5s\ ^1D_2$ transition at 348.977 nm.[34,35] A broadband interference filter centered at 350 nm was utilized to isolate the fluorescence. The fluorescence is detected at 90° to the counterpropagated laser beams with a three-lens telescope imaged through an iris. A photomultiplier tube (Hamamatsu R375) is used in collecting the LIF which is subsequently sent to a gated boxcar sampling module (Stanford Research Systems SR250), and the digitized output is stored and analyzed by a computer. Real time viewing of the photolysis prompt emission and LIF signal are accomplished using a LeCroy model 9360 digital oscilloscope. Reactions were monitored by observing the temporal decay of Pd atoms as a function of O_2 partial pressure. Temporal profiles were collected by measuring the LIF signal at different probe laser delays relative to the photolysis laser. The laser delays were varied by a digital delay generator (Stanford Research Systems DG535) controlled by a computer interfaced through a Stanford Research Systems SR245 computer interface. The trigger source for these experiments was scattered pump laser light incident upon a fast photodiode. LIF decay traces consisted of 200 data points, each point averaged for three laser shots.

The [$Pd(CF_3CO_2)_2$] precursor was entrained in a flow of argon buffer gas. The diluted precursor, buffer gas and O_2 flowed through calibrated mass flow meters and flow controllers (MKS Types 1459C and 0258C, and Matheson models 8102 and 8202−1423) prior to admission to the reaction chamber. Each sidearm window was purged with a slow flow of buffer gas to prevent deposition of metal atoms and other photoproducts. Pressures were measured with MKS Baratron manometers, and chamber temperatures were measured with a thermocouple.

Data Analysis and Results

The decay rates of the ground state (a^1S_0) of Pd as a function of O_2 partial pressure in Ar buffer were investigated at different total pressures at room temperature (294 ± 1 K). A majority of the decay profiles showed growth (i.e., nonexponential behavior) at the beginning of the decays as shown in Figure 1. This behavior is attributed to the relaxation of the higher electronic states to the ground state. In the presence of O_2, the electronically excited states react/relax much more rapidly than the ground state. Thus, slight growth at short laser delays is typically observed for the ground state in the presence of O_2, and exponential decays are observed at longer laser delays. Once the electronically excited states have relaxed, the loss of ground-state Pd is described by the pseudo first-order decay constant, k':

$$k' = 1/\tau = k_d + k_{obs}[O_2]$$

where τ is the first-order time constant for the removal of Pd under the given experimental conditions, k_d is the loss term due to diffusion out of the detection zone and reaction with the precursor, and k_{obs} is the second-order rate constant. Time constants were determined by adjusting the range of the linear regression analysis, i.e., the range did not include the beginning of the decay when growth was present. Typical decays were analyzed after a delay of slightly less than one reaction lifetime and included data for a length of two to three reaction lifetimes. The observed second-order rate constant is determined from the slope of a plot of $1/\tau$ vs $[O_2]$. Typical plots for obtaining the second-order rate constants are presented in Figures 2 and 3. The relative uncertainty (i.e., reproducibility) of the rate constants is estimated at ±10%. The absolute uncertainties are estimated at ±30% and are based on the sum of the statistical scatter in the data, uncertainty in the flow meter, flow controller, and pressure readings, and errors associated with incomplete mixing. Second-order rate constants in argon buffer as a function of temperature and pressure are listed in Table 1. Rate constants above room temperature were only measured at 20 Torr or less. Rate constants above 523 K could not be measured due to thermal decomposition of the palladium(II) trifluoroacetate precursor.

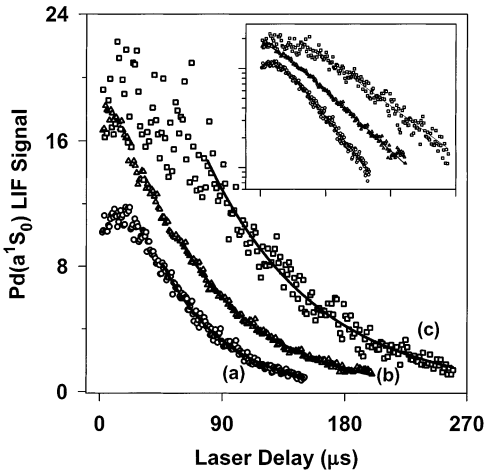

Figure 1. Typical decay curves for $Pd(a^1S_0)$ with added O_2 in argon buffer at 294 ± 1 K; (a) P_{total} = 300.0 Torr, $P(O_2)$ = 77.2 mTorr, τ = 47.6 μs; (b) P_{total} = 20.0 Torr, $P(O_2)$ = 708. mTorr, τ = 64.3 μs. (c) P_{total} = 150.0 Torr, $P(O_2)$ = 68.0 mTorr, τ = 80.4 μs. The solid lines through the data are least-squares fits. The inset is a ln plot of the data.

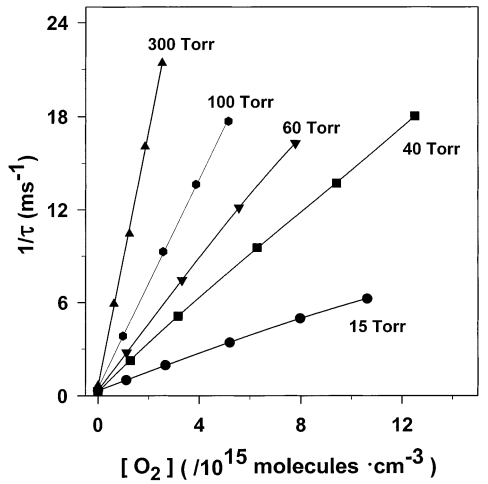

Figure 2. Typical plots for determining k_{obs} for $Pd(a^1S_0) + O_2$ at 294 ± 1 K. The solid line for each set of data is a linear regression fit from which k_{obs} is obtained.

TABLE 1: Second-Order Rate Constants[a] for Pd(a^1S_0) Reacting with O_2.

temp (K)	pressure (Torr)	k_{obs} (10^{-13} molecule^{-1} cm^3 s^{-1})
294[b]	5.0	1.3
	5.0	1.4
	10.0	2.5
	10.0	2.4
	10.0	3.0
	15.0	5.5
	20.0	6.1
	40.0	14.
	60.0	21.
	80.0	27.
	100.0	34.
	150.0	50.
	200.0	60.
	250.0	74.
	300.0	82.
348	10.0	2.0
	20.0	4.2
373	10.0	1.7
	20.0	3.6
398	20.0	3.0
423	10.0	1.2
	20.0	2.2
448	20.0	1.8
473	10.0	0.74
	20.0	1.2
	20.0	1.2
498	20.0	0.89
523	20.0	0.74

[a] Absolute uncertainties are estimated at ±30%. [b] Room-temperature varied from 293 to 295 K.

Discussion

The rate constants in Table 1 are clearly dependent on the total pressure, indicating that the reaction between Pd and O_2 involves recombination (rather than abstraction, in accord with the thermochemical considerations discussed in the introduction):

$$Pd + O_2 (+ Ar) \rightarrow PdO_2$$

To examine this reaction and to extrapolate k_1 outside the experimental pressure and temperature range, we now describe a set of quantum calculations on PdO_2 followed by the application of RRKM theory to reaction 1. The singlet and triplet forms of PdO_2 were investigated using the hybrid density functional/Hartree−Fock B3LYP method from within the Gaussian 98 suite of programs.[36] The molecular geometries were first optimized using the LANL2DZ basis set. This is the standard basis set provided in the Gaussian 98 suite[36] for calculations on post-third-row atoms: the inner electrons on the heavy atoms are treated using effective core potentials, and some relativistic effects are included.[37] The resulting geometries, dipole moments, rotational constants, and vibrational frequencies are listed in Table 2, together with the Pd−O_2 bond energies. Note that these were calculated with respect to neutral Pd and O_2 rather than Pd^+ and O_2^- (in which case they would be larger by 20 kJ mol^{-1} after correcting with the experimental ionization energy of Pd and electron affinity of O_2).

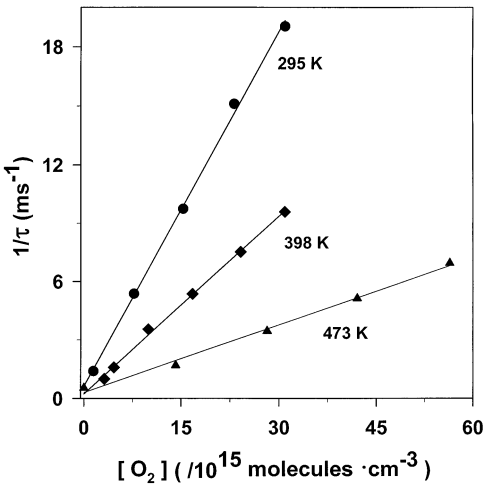

Figure 3. Plots for determining k_{obs} for Pd(a^1S_0) + O_2 at 20.0 Torr at 294, 398, and 473 K. The solid line for each set of data is a linear regression fit from which k_{obs} is obtained.

Table 2 shows that the most stable form of PdO_2 is the bent triplet dioxide. The Mulliken population of the Pd atom (+0.25) indicates that the interaction with the O_2 does not involve a complete electron transfer, hence the relatively small binding energy. A scan of the triplet potential energy surface reveals that there are no significant barriers to forming $PdO_2(^3A'')$. However, the other forms of PdO_2, particularly where the Pd atom inserts into the O_2 to form OPdO either as a linear molecule with triplet spin or a bent dioxide with singlet spin, are very weakly bound or metastable with respect to Pd + O_2. Therefore, we conclude that $PdO_2(^3A'')$ is likely to be the only product of reaction 1 over the experimental temperature range employed here.

There does not appear to be any experimental data available with which to compare these theoretical predictions on PdO_2. Although the LANL2DZ basis set is too small to yield highly quantitative results, we note that at the B3LYP/LANL2DZ level the calculated ionization energy of Pd is 829 kJ mol^{-1} and the electron affinity of O_2 is 46 kJ mol^{-1}, which compare very satisfactorily with the experimental values of 804 and 41 kJ mol^{-1}, respectively. Inspection of Table 2 shows that the PdO_2 molecules have large dipole moments (with the obvious exception of linear $OPdO(^3\Sigma_g^-)$), indicating a significant degree

TABLE 2: Optimized Geometries and Molecular Parameters for the Most Stable Triplet and Singlet Forms of PdO_2, Calculated at the B3LYP/LANL2DZ Level of Theory[a]

species	geometry	dipole moment[b]	rotational constants[c]	vibrational frequencies[d]	D_0(Pd−O_2)[e]
$PdO_2(^3A")$	r(Pd−O) = 2.05 Å; r(O−O) = 1.32 Å ∠Pd−O−O = 110.7°	3.5	56.9, 3.53, 3.32	128, 360, 1194	95
$PdO_2(^1A_1)$ C_{2v} symmetry	r(Pd−O) = 2.08 Å; r(O−O) = 1.40 Å ∠O−Pd−O = 39.2°	4.6	32.3, 5.39, 4.62	221, 384, 1058	29
$OPdO(^3\Sigma_g^-)$ linear	r(Pd−O) = 1.92 Å	0.0	4.30	53, 100, 496, 564	−22
$OPdO(^1A_1)$ C_{2v} symmetry	r(Pd−O) = 1.81 Å; r(O−O) = 3.21 Å ∠O−Pd−O = 125.0°	4.61	29.5, 6.14, 5.08	177, 749, 783	−147

[a] The molecules are listed in order of decreasing Pd−O_2 bond strength. [b] In Debye (= 3.336 × 10^{-30} Cm). [c] In GHz. [d] In cm^{-1}. [e] In kJ mol^{-1}.

of charge transfer between Pd and O_2. A satisfactory calculation of the relative energies of the neutral and ionic dissociation limits therefore provides confidence that this theoretical method describes the Pd−O_2 system well enough for the calculations that follow.

We now apply RRKM theory to reaction 1, using a master equation (ME) formalism[38] which we have recently applied to recombination reactions of metallic species.[23,39] The reaction is considered to proceed via the mechanism:

$$Pd + O_2 \rightarrow PdO_2^* \quad (1.1)$$

$$PdO_2^* \rightarrow Pd + O_2 \quad (1.\text{-}1)$$

$$PdO_2^* + Ar \rightarrow PdO_2 + Ar \quad (1.2)$$

The energy of the adduct PdO_2 was first divided into a contiguous set of grains (width 30 cm^{-1}), each containing a bundle of rovibrational states of average energy, E_i. Each grain was then assigned a set of microcanonical rate coefficients for dissociation, $k^{-1}(E_i)$. The ME describes the evolution with time of the grain populations

$$\frac{d}{dt}\rho_i(t)\ \omega \sum_j P_{ij}\rho_j(t) - \omega\rho_i(t) - k^{-1}(E_i)\rho_i(t) + R_i \quad \text{(II)}$$

where R_i is the rate of population of $PdO_2(E_i)$ via reaction 1.1, ω is the frequency of collisions between PdO_2^* and Ar, and P_{ij} is the probability of transfer of PdO_2 from grain j to grain i on collision with Ar. The individual P_{ij} were estimated using the exponential down model,[40] with the average energy for downward transitions ($i < j$), $\langle\Delta E\rangle_{down}$, an adjustable parameter between 150 and 300 cm^{-1} for Ar.[40] For upward transitions where $j > i$, P_{ij} was calculated by detailed balance. To use the ME to simulate irreversible stabilization of PdO_2 via reaction 1.2, an absorbing boundary was set 24 kJ mol^{-1} below the energy of the reactants, so that collisional energization from the boundary to the threshold was highly improbable. The rate of population of grain i, R_i, is given by detailed balance between reactions 1.1 and 1.-1:

$$R_i = k_{rec,\infty}[Pd][O_2]\eta_i \quad \text{(III)}$$

where $k_{rec,\infty}$ is the limiting high-pressure association rate coefficient (reaction 1.1) and

$$\eta_i = \frac{k_{-1,i}\, f_i}{\sum_i k_{-1,i} f_i} \quad \text{(IV)}$$

where f_i is the equilibrium Boltzmann distribution of $PdO_2(E_i)$.

The microcanonical rate coefficients for dissociation of PdO_2 were determined using inverse Laplace transformation,[38] which links $k_{-1}(E_i)$ directly to $k_{rec,\infty}$. In the present case, $k_{rec,\infty}$ was expressed in the Arrhenius form $A^\infty \exp(-E^\infty/RT)$. The microcanonical rate coefficient for dissociation is then given by

$$k_{-1}(E_i) = \frac{A^\infty(2\pi\mu)^{3/2}}{N(E_i)\Gamma(1.5)h^3}\int_0^{E_i - E^\infty - \Delta H_0^\circ} N_p(x)[(E_i - E^\infty - \Delta H_0^\circ) - x]^{0.5}\, dx \quad \text{(V)}$$

where the density of states of PdO_2 at energy E_i, $N(E_i)$, was calculated using a combination of the Beyer−Swinehart algorithm for the vibrational modes (without making a correction for anharmonicity) and a classical densities of states treatment for the rotational modes; $N_p(E_i)$ is the convoluted density of states of Pd and O_2; ΔH_0° is the Pd−O_2 bond energy; and μ is the reduced mass of Pd and O_2. The ME was expressed in matrix form and then solved to yield k_{calc}, the bimolecular recombination rate constant at a specified pressure and temperature.

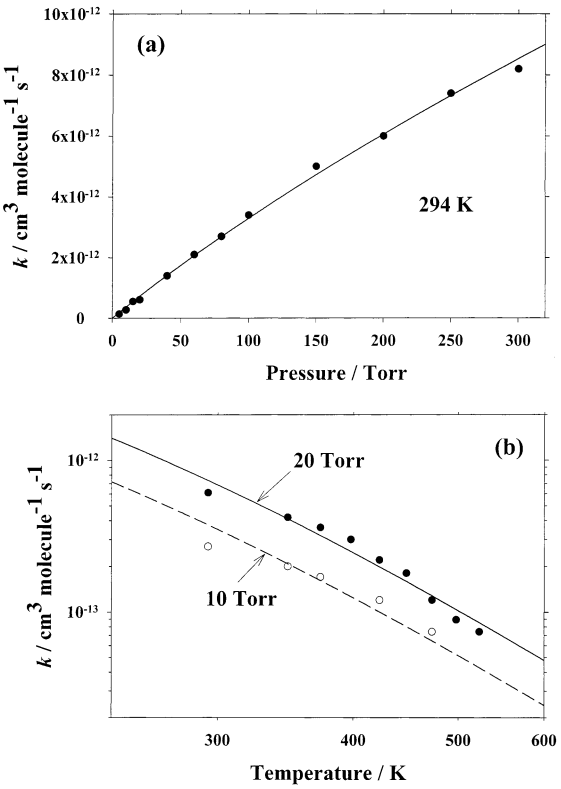

Figure 4. Plots of $k(Pd + O_2)$ versus (a) pressure at 294 K, and (b) temperature at pressures of 10 and 20 Torr. The points are the measured k_{obs}, and the lines are RRKM fits.

To fit k_{calc} to the experimental data in Table 1, six adjustable parameters were allowed. These were the Arrhenius parameters A^∞ and E^∞, which define $k_{rec,\infty}$; the parameters σ and ϵ/k describing the intermolecular potential between PdO_2 and Ar, from which ω was calculated; the average energy for downward transitions, $\langle\Delta E\rangle_{down}$; and α, which defines the (small) T^α dependence of $\langle\Delta E\rangle_{down}$. These parameters were varied in a simple grid search to minimize χ^2, defined as

$$\chi^2 = \sum_i^N \left(\frac{k_{obs,i} - k_{calc,i}}{\sigma_i}\right)^2 \quad \text{(VI)}$$

i.e., the sum over N experimental points of the squared difference between the measured $k_{obs,i}$ (with uncertainty σ_i) and the modeled value $k_{calc,i}$. The best fit parameters are $A^\infty = 2.52 \times 10^{-10}$ cm^3 $molecule^{-1}$ s^{-1}, $E^\infty = 576$ J mol^{-1}, $\sigma = 3.04$ Å, $\epsilon/k = 270$ K, $\langle\Delta E\rangle_{down} = 230$ cm^{-1}, and $\alpha = -0.40$. The largest deviation between k_{calc} and k_{obs} was 20.5%, with an average deviation of 7.6%. This satisfactory fit of RRKM theory to the experimental data over a range of pressure and temperature is illustrated in Figure 4.

Fitting RRKM theory to the experimental data can also be used to constrain the value of $D_0(Pd-O_2)$. If we assume that the parameters σ, ϵ/k, and $\langle\Delta E\rangle_{down}$ remain within their expected ranges (2−3.5 Å, 200−300 K, and 150−300 cm^{-1}, respectively), and that the lowest vibrational frequency of PdO_2 is allowed to vary from 80 to 160 cm^{-1} compared with the

calculated value of 129 cm^{-1} (Table 2), then $D_0(Pd-O_2)$ should lie between 80 and 155 kJ mol^{-1}. This indicates that the bond energy of 95 kJ mol^{-1} calculated at the B3LYP/LANL2DZ level must be a reasonably good estimate, even though the basis set is relatively small and should not in general yield good quantitative results. It should be noted that despite the bond between Pd and O_2 being comparatively weak, the lifetime of PdO_2 against thermal dissociation at the highest temperature (523 K) employed in this study should still be about 0.4 s at a pressure of 20 Torr, so that thermal dissociation would not have affected the observed kinetic decays of atomic Pd.

To provide a simple expression for extrapolating k_{calc} over a larger range of temperature (200−600 K) and pressure (10^{-3}−10^3 Torr), we have fitted the RRKM results to the Lindemann expression modified by a broadening factor F_c:

$$k_{calc} = \frac{k_{rec,0}[M]}{1 + \frac{k_{rec,0}[M]}{k_{rec,\infty}}} F_c^{\,K}$$

where

$$K = \frac{1}{\left\{1 + \left(\log_{10}\left(\frac{k_{rec,0}[M]}{k_{rec,\infty}}\right)\right)^2\right\}} \qquad \text{(VII)}$$

where $k_{rec,0} = 1.09 \times 10^{-30} (T/300\ K)^{-2.76}$ cm^6 $molecule^{-2}$ s^{-1}, $k_{rec,\infty} = 2.52 \times 10^{-10} \exp(-69.3/T)$ cm^3 $molecule^{-1}$ s^{-1}, and $F_c = 0.61$. The uncertainty involved in using expression VII to extrapolate k_{calc} outside the experimental range of temperature and pressure was estimated using a Monte Carlo sampling procedure that we have described in detail previously.[23] It takes account of the fact that the six fitted RRKM parameters are not all independent of each other. The 2σ uncertainty in k_{calc} is ±65% at 200 K, ±34% at 400 K, and ±42% at 600 K, over the pressure range 10^{-3}−10^3 Torr.

Acknowledgment. This research was supported by the Camille and Henry Dreyfus Foundation, Inc.

References and Notes

(1) Brown, A.; Husain, D. *Can. J. Chem.* **1976**, *54*, 4.
(2) Wiesenfeld, J. R.; Yuen, M. J. *J. Phys. Chem.* **1978**, *82*, 1225.
(3) Nien, C.-F.; Plane, J. M. C. *J. Chem. Phys.* **1991**, *94*, 7193.
(4) Garland, N. L.; Nelson, H. H. *Chem. Phys. Lett.* **1992**, *191*, 269.
(5) Fontijn, A.; Bajaj, P. N. *J. Phys. Chem.* **1996**, *100*, 7085.
(6) LePicard, S. D.; Canosa, A.; Travers, D.; Chastaing, D.; Rowe, B. R.; Stoecklin, T. *J. Phys. Chem.* **1997**, *101*, 9988.
(7) Campbell M. L. *Chem. Phys. Lett.* **1998**, *294*, 339, and references therein.
(8) Campbell, M. L. *J. Phys. Chem. A* **1998**, *102*, 892.
(9) Campbell, M. L. *J. Phys. Chem. A* **1999**, *103*, 7274.
(10) Campbell, M. L. *Chem. Phys. Lett.* **2000**, *330*, 547.
(11) Brown, C. E.; Mitchell, S. A.; Hackett, P. A. *J. Phys. Chem.* **1991**, *95*, 1062.
(12) Plane, J. M. C. In *Gas-Phase Metal Reactions*; Fontijn, A., Ed.; Elsevier: Amsterdam, 1992; p 29.
(13) Vinckier, C.; Christiaens, P.; Hendrickx, M. In *Gas-Phase Metal Reactions*; Fontijn, A., Ed.; Elsevier: Amsterdam, 1992; p 57.
(14) Campbell, M. L. *J. Chem. Soc., Faraday Trans.* **1996**, *92*, 4377.
(15) Campbell, M. L. *J. Phys. Chem. A* **1997**, *101*, 9377.
(16) Campbell, M. L. *J. Chem. Soc., Faraday Trans.* **1998**, *94*, 353.
(17) Campbell, M. L. *Laser Chem.* **1998**, *17*, 219.
(18) Vinckier, C.; Christiaens, P. *Bull. Soc. Chim. Belg.* **1992**, *101*, 10.
(19) Nien, C.-F.; Rajasekhar, B.; Plane, J. M. C. *J. Phys. Chem.* **1993**, *97*, 7, 6449.
(20) Vinckier, C.; Remeysen, J. *J. Phys. Chem.* **1994**, *98*, 10535.
(21) Helmer, M.; Plane, J. M. C. *J. Chem. Soc., Faraday Trans.* **1994**, *90*, 395.
(22) Vinckier, C.; Helaers, J. *J. Phys. Chem. A* **1998**, *102*, 8333.
(23) Campbell, M. L.; Plane, J. M. C. *J. Phys. Chem. A* **2001**, *105*, 3515.
(24) Plane, J. M. C. *Int. Rev. Phys. Chem.* **1991**, *10*, 55.
(25) McNeil, W. J.; Murad, E.; Plane, J. M. C. Models of Meteoric Metals in the Atmosphere. In *Meteors in the Earth's Atmosphere*; Murad, E., Williams, I. P., Eds.; Cambridge University Press: Cambridge, 2002; p 265.
(26) Fontijn, A.; Blue, A. S.; Narayan, A. S.; Bajaj, P. N. *Combust. Sci. Technol.* **1994**, *101*, 59.
(27) Tsuji, J. *Palladium Reagents and Catalysts Innovations in Organic Synthesis*; Wiley: New York, 1995.
(28) Bare, W. D.; Citra, A.; Chertihin, G. V.; Andrews, L. *J. Phys. Chem. A* **1999**, *103*, 5456 and references therein.
(29) Blomberg, M. R. A.; Siegbahn, P. E. M.; Svensson, M. *J. Am. Chem. Soc.* **1992**, *114*, 6095.
(30) Carroll, J. J.; Haug, K. L.; Weisshaar, J. C.; Blomberg, M. R. A.; Siegbahn, P. E. M.; Svensson, M. *J. Phys. Chem.* **1995**, *99*, 13955.
(31) Hildenbrand, D. L.; Lau, K. H. *Chem. Phys. Lett.* **2000**, *319*, 95.
(32) Wagman, D. D.; Evans, W. H.; Parker, V. B.; Schumm, R. H.; Halow, I.; Bailey, S. M.; Churney K. L.; Nuttall, R. L. *J. Phys. Chem. Ref. Data* **1982**, *11*, Suppl. 2.
(33) Campbell, M. L.; McClean, R. E. *J. Chem. Soc., Faraday Trans.* **1995**, *91*, 3787.
(34) Meggers, W. F.; Corliss, C. H.; Scribner, B. F. *Tables of Spectral-Line Intensities, Part I Arranged by Elements*; NBS Mono. 145, U.S. Government Printing Office, Washington, DC, 1975.
(35) Moore, C. E. Atomic Energy Levels as Derived from the Analysis of Optical Spectra. *Natl. Stand. Ref. Data Ser. (U.S., Natl. Bur. Stand.)* 1971, NSRDS-NBS 35, Vol. III.
(36) Frisch, M. J.; Trucks, G. W.; Schlegel, H. B.; Scuseria, G. E.; Robb, M. A.; Cheeseman, J. R.; Zakrzewski, V. G.; Montgomery, J. A., Jr.; Stratmann, R. E.; Burant, J. C.; Dapprich, S.; Millam, J. M.; Daniels, A. D.; Kudin, K. N.; Strain, M. C.; Farkas, O.; Tomasi, J.; Barone, V.; Cossi, M.; Cammi, R.; Mennucci, B.; Pomelli, C.; Adamo, C.; Clifford, S.; Ochterski, J.; Petersson, G. A.; Ayala, P. Y.; Cui, Q.; Morokuma, K.; Malick, D. K.; Rabuck, A. D.; Raghavachari, K.; Foresman, J. B.; Cioslowski, J.; Ortiz, J. V.; Baboul, A. G.; Stefanov, B. B.; Liu, G.; Liashenko, A.; Piskorz, P.; Komaromi, I.; Gomperts, R.; Martin, R. L.; Fox, D. J.; Keith, T.; Al-Laham, M. A.; Peng, C. Y.; Nanayakkara, A.; Gonzalez, C.; Challacombe, M.; Gill, P. M. W.; Johnson, B.; Chen, W.; Wong, M. W.; Andres, J. L.; Gonzalez, C.; Head-Gordon, M.; Replogle, E. S.; Pople, J. A. Gaussian 98, Revision A.7, Gaussian, Inc., Pittsburgh, PA, 1998.
(37) Foresman, J. B.; Frisch, A. *Exploring Chemistry with Electronic Structure Methods*; Gaussian, Inc., Pittsburgh, PA, 1996.
(38) De Avillez Pereira, R.; Baulch, D. L.; Pilling, M. J.; Robertson, S. H.; Zeng, G. *J. Phys. Chem.* **1997**, *101*, 9681.
(39) Rollason, R. J.; Plane, J. M. C. *Phys. Chem. Chem. Phys.* **2000**, *2*, 2335.
(40) Gilbert, R. G.; Smith, S. C. *Theory of Unimolecular and Recombination Reactions*; Blackwell: Oxford, 1990.